



Wear response of non-asbestos brake pad composites reinforced with walnut shell dust

Gülşah Akıncioğlu¹ · Sıtkı Akıncioğlu¹ · Hasan Öktem² · İlyas Uygur³

Received: 10 December 2018 / Revised: 17 December 2019 / Accepted: 19 January 2020 / Published online: 30 January 2020
© Australian Ceramic Society 2020

Abstract

With automobile numbers continuing to increase, competition among manufacturers of brake pads is also increasing along with the search for additives to serve as alternatives to the materials presently being used. In addition to the cost of the additives used, another important consideration in choosing materials is that they should be safe for the environment and human health. This study investigated the effect on braking performance of brake pads produced using walnut shell powder as a natural additive material. Two different types of brake pad samples were produced using 3.5 (2A) and 7% (2B) walnut shell dust in the contents. A commercial Clio brake tip was used as the reference (CO). The produced brake pads were subjected to thermal conductivity, friction wear, density, hardness and water and oil absorption tests and microstructure analysis. A Chase type device was used for wear friction tests, and the results were obtained according to SAE-J661 (Brake Lining Quality Test Procedure) standards. The experimental data were compared with those of the commercial brake pads, and the performances of the natural additive brake pads were evaluated. The addition of walnut shell was shown to be compatible within the composition and exhibited a positive effect on the friction coefficient.

Keywords Brake pads · Walnut shell dust · Porosity · Friction and wear test · Chase type device

Introduction

Modern brake pad materials have much in common with primitive ropes. Along with evolving automotive technology, many studies have been aimed at producing high performance, cheap, environmentally friendly brake pads that do not cause harmful effects on health [1, 2]. The performance of the braking system depends on the friction behaviour between the rotating disk and the brake pad. Brake friction materials are heterogeneous, and improved formulations vary in

physical, mechanical and chemical properties. In order to achieve an optimal braking performance, composites are formed by using many materials in combination [3]. Thousands of different materials have been used commercially as brake components [4, 5]. They are classified as binders, reinforcing materials, fillers and friction modifiers. The friction and wear properties of a developed formulation cannot be predicted based on the physical and mechanical properties of the materials [6, 7]. Due to the harmful effects of materials such as asbestos, in recent years, there have been significant changes in pad materials. A great effort is being made to develop high performance, environmentally friendly brake pads [8, 9]. Organic materials such as wollastonite, vermiculite, mica, basalt fibre, chopped glass fibre, ceramic fibre, polyacrylonitrile, rock wool, polyester and aramid fibres used in place of asbestos have similar performance characteristics [10]. In addition, natural and agricultural residues and wastes have begun to be used as new and inexpensive materials in the development of brake pads [11]. In determining the composition, factors that need to be taken into consideration include the type of vehicle to be used, the type of primer needed, the nature and cost of the materials to be used, the manufacturing cost and the health and environmental impact [12]. Wastes are

✉ Gülşah Akıncioğlu
gulsahakincioglu@gmail.com; gulsahakincioglu@duzce.edu.tr

Sıtkı Akıncioğlu
sitkiakincioglu@gmail.com

¹ Department of Machine Design and Construction, Düzce University, Düzce, Turkey

² Department of Machine and Metal Technologies, Kocaeli University, 41800 İzmit, Kocaeli, Turkey

³ Department of Mechanical Engineering, Düzce University, Düzce, Turkey

produced abundantly in the world and are a hazard to human as well as environmental health. Violet sea snail shell is an agricultural waste. Aku et al. used periwinkle shell as an alternative to asbestos-free brake pads. The results confirmed that periwinkle shell could be used as a material for brake pad production [13]. Ibadode et al. used palm kernel shell to produce asbestos-free brake tips. The results suggested that palm kernel shell might replace asbestos as friction material [8, 14, 15]. Walnut shells have various industrial uses, such as for firewood, in chipboard manufacture, as a cleaning material in the chemical and metal industries, for charcoal and more. In some studies, it has also been used as an additive in brake pads. Qui et al. [16] found that the effect of the walnut shell powder they use in their work has proven to be very advantageous in balancing the friction coefficient of the friction materials studied and increasing the wear resistance. Approximately 120,000 tons of walnut shell is produced annually in Turkey alone. Due to its chemical composition, walnut shell can be used as a friction modifier in brake pads. The shell rate in walnuts ranges from 40 to 60% on average, depending on the type of walnut. The use of walnut shell as a friction modifier in brake pads would increase its use and industrial value.

In this study, walnut shell dust, which is harmless to the environment and health, was used as additive material in brake pads. A Renault Clio brake pad produced with natural additives along with the pads produced with walnut shell were subjected to density and hardness tests, microstructure analysis and thermal conductivity and friction wear testing. The obtained experimental data were evaluated for the performance of the walnut shell additive pads and the commercial reference brake pad with natural additives.

Experimental procedure

The elemental analysis

Walnut shell (Fig. 1) was used as the friction modifier in the composition of the brake pads. The chemical composition of the walnut shell has about 49% lignin, 47% holocellulose,

26% cellulose and other ingredients. In addition to walnut shell, brass chips and graphite were used as friction modifiers; steel wool, rock wool and kevlar as reinforcing fibres; phenolic resin and rubber dust as binders and vermiculite, calcium hydroxide and baryte as filling material.

The physical properties of the walnut shell dust used in the brake pads are given in Table 1.

The composition of the brake pads is given in Table 2.

Brake pad samples were manufactured by following certain procedures using the prepared components. The process for pressing the brake pads is given in Fig. 2.

Brake pads were produced by hot pressing. Plates were cleaned by blasting (Step 1). The moulds were cleaned (Step 2). The brake pad composition was then placed in the moulds (Step 3). The plates were then placed in the moulds (Steps 4–6). The top cover was closed onto the mould and made ready for moulding (Step 7). The load and temperature applied during the pressing of the brake pads is important for properly obtaining the pad. The production of the pads was carried out at a pressure of 100 kg/cm² at 180 °C for 6 min (Fig. 2, Step 8). During pressing, the air was withdrawn by retracting the press mould three times for 10 s. Otherwise, porosity may form at the beginning, or the materials forming the liner composition may not be able to hold together.

Physical behaviour analysis

After the brake pads were manufactured, microstructure and energy dispersive X-ray (EDX) analyses (Quanta FEG 250, Hillsboro, Oregon), density, water absorption, oil absorption, thermal conductivity tests (C-Therm TCI model device, New Brunswick, Canada) and hardness were performed to evaluate their performance. Friction wear tests were carried out on a Chase type device (BL-600-CT), and the wear rate results were analysed.

In this study, the hardness measurements of the brake pads were made using a Shore D (Durometer) measuring device [17, 18], and the average of the values from five different points on the surface of the pad was calculated. The hardness measurements of the brake pads were made in accordance with SAE J2654 standard (Hardness of Brake Lining).

Fig. 1 a Walnut shell; b SEM image of walnut shell dust

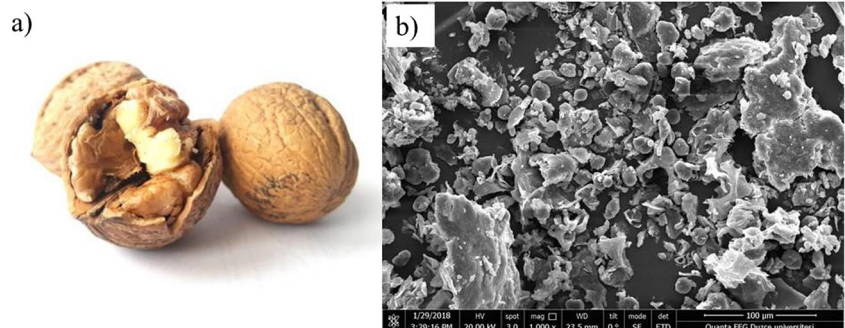


Table 1 Physical properties of walnut shell dust

	Property	Walnut shell
1	Density (g/cm ³)	0.368
2	Thermal conductivity (W/mK)	1.112
3	Particle size (µm)	289.08

The density values of pads depend on the composition used, the powder dimensions, the moulding method and the heat treatment performed [19]. The density test was carried out on the brake pad samples using the Archimedes’ principle (Redmag PS360.R2 model) according to ASTM D792 (Standard Test Methods for Density and Specific Gravity (Relative Density) of Plastics by Displacement) [11, 20–23]. For measuring the density of the pads, a density kit with a precision scale was used. The samples were cut to size to fit the heel. The density of the sample was measured according to the Archimedes’ principle by placing the sample in a beaker containing pure water. The density was calculated using the formula in Eq. (1).

$$\text{Density (g/cm}^3\text{)} = \frac{\text{Dry weight (g)}}{\text{Dry weight (g)} - \text{Wet weight (g)}} \quad (1)$$

The water and oil absorption tests, shown in Fig. 3, were applied to observe the changes produced in the new brake compositions in water and oil environments. The dimensional changes of the samples which were kept in water and oil for 24 h were measured using a micrometre. The weight changes

Table 2 Weight ratios of additives used in the pads

	No	Powder material	2A	2B	CO
<i>Joint additives</i>	1	Steel wool	15–20	15–20	15–20
	2	Rock wool	3–6	3–6	3–6
	3	Kevlar	0.5–2	0.5–2	0.5–2
	4	Graphite	5–7	5–7	5–7
	5	Phenolic resin	6–8	6–8	6–8
	6	Vermiculite	6–8	6–8	6–8
	7	Brass chip	4–6	4–6	4–6
	8	Calcium hydroxide	7–9	7–9	7–9
	9	Zirconium silicate	3–5	3–5	3–5
	10	Sulphur	0.5–1	0.5–1	0.5–1
	11	Black iron oxide	1–3	1–3	1–3
	12	Rubber powder	4–6	4–6	4–6
	13	Baryte	6–8	6–8	6–8
	14	Rubber	2–4	2–4	2–4
	15	Chalcopyrite	6	6	6
	16	Quartz + mica	4.5	4.5	4.5
<i>Variable additives</i>	17	Petrocoke	3.5	–	7
	18	Walnut shell dust	3.5	7	–

were measured by precision scales, and the hardness changes were measured with the Shore D hardness tester (Fig. 3). These tests were performed according to ASTM D 570–98 standard (Standard Test Method for Water Absorption of Plastics) [24]. The brake pads were measured in terms of hardness, weight, width, length and thickness after immersion in water and oil for 24 h.

The C-therm TCI analyser was used for the measurement of the thermal conductivity coefficient of the brake pads produced in different composites. The thermal conductivity measurements of the brake pads were made in accordance with ASTM 1114–98 (“Standard Test Method” for “Thin Heater Apparatus”).

Morphological analysis

Microstructural investigations were carried out to determine the homogeneous distribution of the elements in the new compositions and their compatibility with each other. The samples prepared for the *scanning electron microscopy* (SEM) (Quanta FEG 250, Hillsboro, Oregon) images were covered with gold, and SEM images of the samples were taken in backscatter mode. The prepared samples are shown in Fig. 4.

The purpose of the acetone extractions test was to detect the organic materials in the pads and to see whether or not the resin was cured. Acetone tests are usually made on two different sites on the sample. If there is a great difference between them, the material does not homogeneously mix or homogeneously cure. The acetone test was carried out according to ASTM 494–04 standard (Standard Specification for Chemical Admixtures for Concrete) [25].

Mechanical behaviour analysis

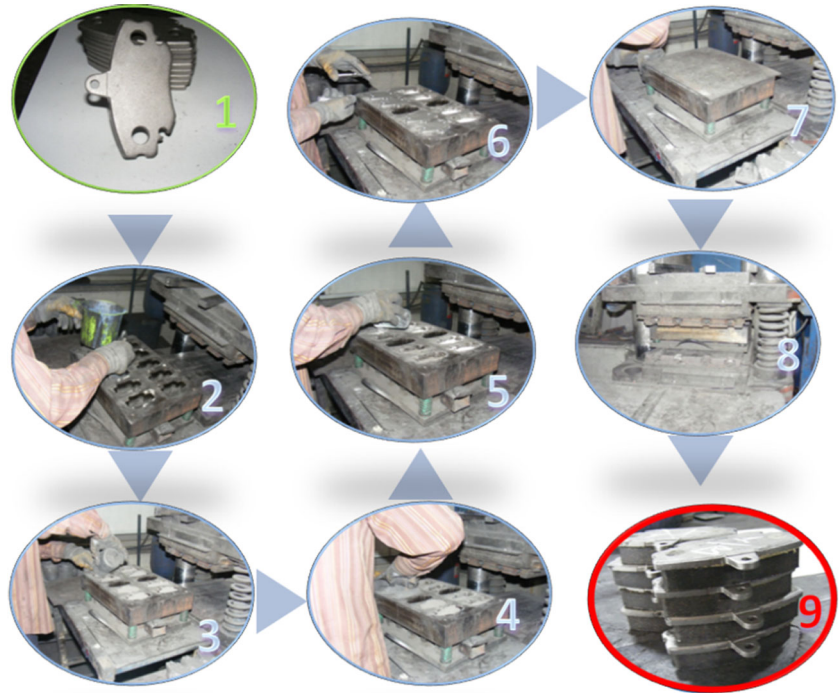
The friction-wear performance of the prepared samples was tested based on SAEJ661 [26] by using the Chase friction test machine (BL-600-CT) (Balatacilar Balatacilik Co. Ltd.). In this machine, the counter face is a cast iron drum with an inner diameter of 30 cm. For friction testing, the surface area of the specimens was square in shape with dimensions of 25.4 × 25.4 × 40 mm. The speed of the drum was 411 rpm and the maximum applied load was 68 kg.

Results and discussion

Morphological analysis

Microstructure images were examined to determine the homogeneous dispersion of the prepared samples, i.e. if the natural additions to 2A and 2B were homogeneously dispersed. In addition, the distribution of the walnut shell in the composition was also examined. Figure 5 shows the EDX analysis of

Fig. 2 Pad manufacturing process



the 2B sample with walnut shell addition. The additives forming the composition and the distribution of these substances in the composition are seen in the EDX analysis. The EDX analysis from the SEM view shows the various sizes and shapes of chalcopryrite, vermiculite, rock wool, wollastonite, walnut shell, steel wool, calcium hydroxide, silica and barium sulphate fragments in the microstructure. The structure of the added walnut shell dust in the composite was found to be fibrous.

Figure 6 gives the microstructural images of the naturally reinforced 2A and 2B and commercial brake pads. The walnut shell dust was homogeneously dispersed and appears in fibre

form in the microstructure. Figure 6a shows a SEM image of the 2A sample (3.5% walnut shell addition). It can be seen that the 2A sample has a tighter structure than the 2B sample. It was understood that the porosity increases seen in the SEM image of 2B (7% walnut shell) were directly proportional to the water and oil absorption rates (Fig. 6b). As the porosity increased in the 2B sample, the water and oil absorption rates increased. It was also seen that the walnut shell dust fibres in the 2B sample were more compact than in the 2A sample. The microstructural images of the 2A and 2B brake pads with natural additives and the CO showed the homogeneous distribution. Moreover, in the image in Fig. 6c, the commercial pad microstructure is seen to be more tightly structured than the others, which can also be explained by the fact that the density was high.

Deformation occurs on brake pad surfaces during friction and due to the heterogeneous nature of brake pads, some abrasions may cause excessive wear. The pores on the lining of the materials are broken by the adhesion mechanism and non-adherent regions form plateaus 1–2 μm high. Figure 7 shows the worn surfaces of the friction materials after friction testing (same maximum scale of friction coefficient and force). The friction materials reinforced with walnut shell showed a

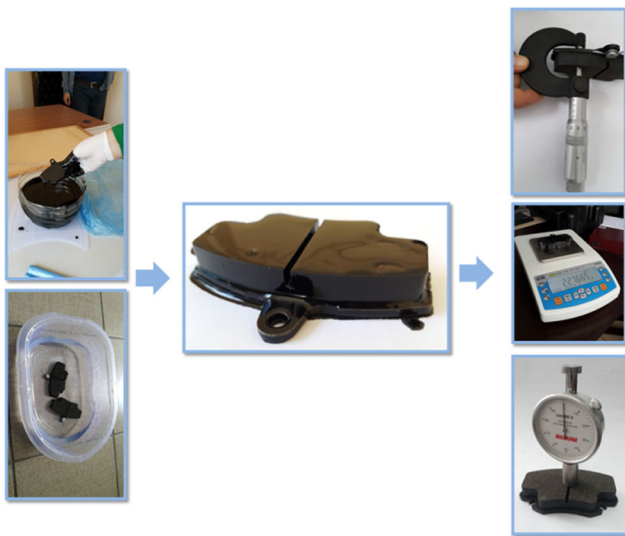
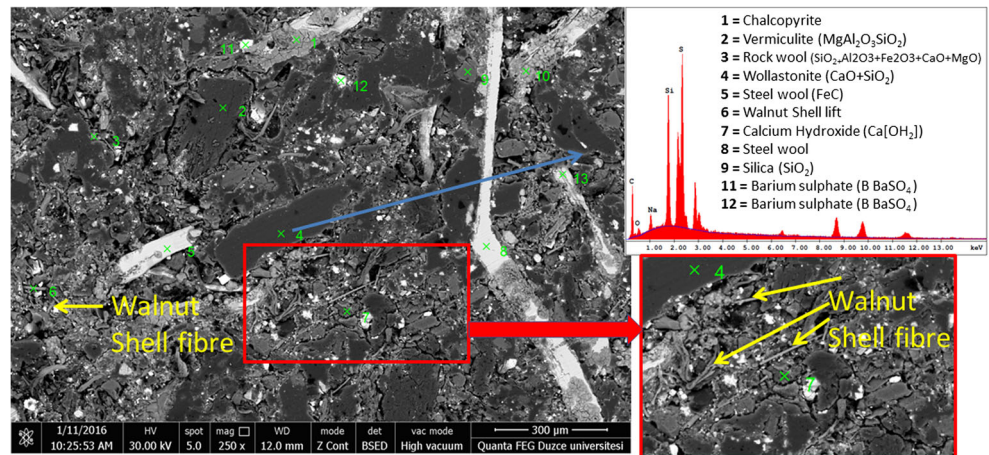


Fig. 3 Brake pad water and oil absorption process



Fig. 4 Samples for SEM images

Fig. 5 EDX analysis of sample 2B



smooth friction film. The most abrasion was found in the commercial pad (CO), where abrasive particles such as zirconium and iron dust were clearly seen to form the abrasive grinding mechanism [27]. Wear traces and surface abrasions were observed in 2A, although the surface of the 2A sample had less evidence of wear than the other pads. Layers adhering to the 2B specimen caused plateaus to form. By increasing the amount of walnut shell, the friction modifier ratio in the composition was also increased. Thus, the trace of wear was reduced due to the formation of the abrasion film on the surface. In addition, iron oxide and steel wool transferred from the disk to the brake pin on the specimens were also detected. Steel wool formed a friction layer containing iron on the friction surface. These layers came in contact with air during friction

to form iron oxide. These particles occurring during friction played a part in the wear of the brake pad [28].

Physical behaviour analysis

The density of brake pads is directly related to the density of the materials forming the contents and the proportions of the different materials. By increasing the amount of high-density material in the composition, the density of the brake pad is also increased. The density value of the commercial pad was measured as 2.470 g/cm³ (Table 4). The density decreased when the walnut shell contribution ratio was increased to 7% in the 2B sample. The increase in the percentage of walnut shell in the composition reduced the density of the brake pad.

Fig. 6 Microstructure images: a 2A; b 2B; c CO

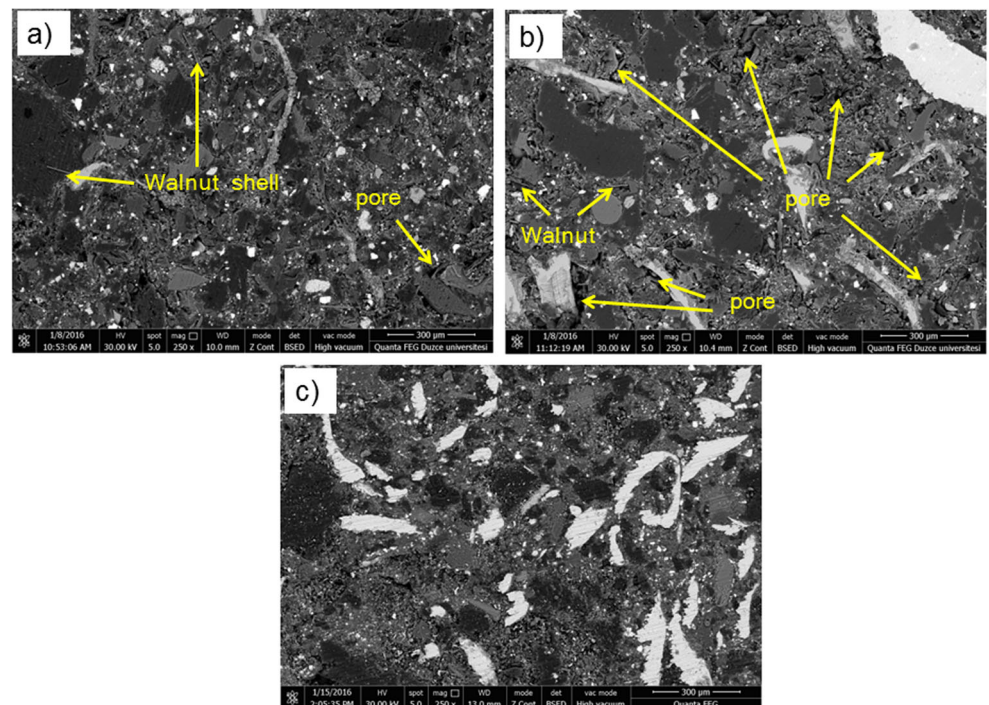
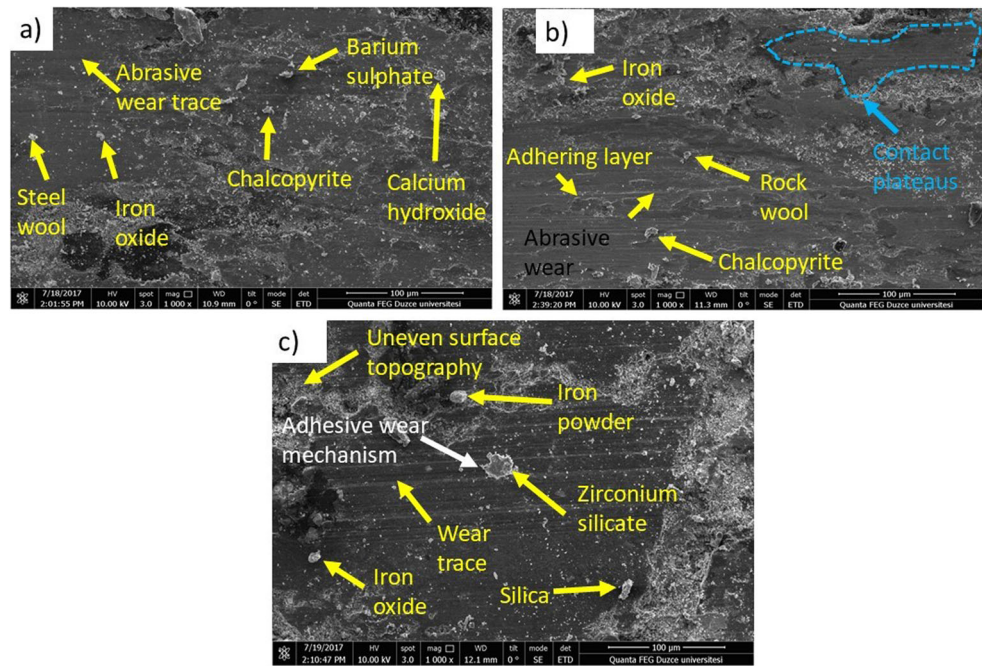


Fig. 7 SEM images of brake pad worn surfaces: **a** 2A; **b** 2B; **c** CO



Walnut powder appears to be one of the lowest density materials among the density values of the powder materials contained in the composition. Increasing the density of the brake pad reduces the porosity. When the microstructure of the 2D sample with the lowest density was examined (Fig. 6b), the micropores were clearly visible. The CO sample, having the lowest water and oil absorption rates, had the highest density [29, 30]. It can be said that the density values of all samples were close to that of the commercial pad. The resulting density measure values were consistent with those of the literature [31]. Yawas et al. also found that as the size of the periwinkle shell increased, the density of the brake pads produced with the agricultural waste periwinkle shell decreased [32].

The thermal conductivity of the composites plays an important role in the performance of brake pads. Low thermal conductivity due to overheating weakens the tribo surface, causes deterioration of the organic components and adversely affects braking ability. On the other hand, extremely high thermal conductivity causes adverse effects on the brake fluid. For these reasons, it is desirable to obtain an optimum thermal conductivity by adjusting the content of the composite metallic fillers [33]. According to ASTM-E1461–01, the thermal conductivity test value should be at most $2.33 \text{ W/m}^2\cdot\text{K}$ ($2 \text{ kcal/h}\cdot\text{m}^2\cdot^\circ\text{C}$). According to the thermal conductivity results, the highest thermal conductivity value ($1.56 \text{ W/m}^2\cdot\text{K}$) was found in the 2A sample (Table 4). These results are within the limits of the standard for thermal conductivity. Increasing the ratio of walnut shell reduced the thermal conductivity. This indicated that the thermal conductivity value of the walnut shell was low.

Car brakes under actual use conditions are obliged to work in environments such as rain, dust and oil. Water and oil affect the friction performance by forming a film between the disk and the pad during braking [34]. It is important that the brake pads do not change much under all these conditions and that their performance is sustainable. Hardness and dimensional integrity should not change much in an oil and water environment. In water and oil environments, friction composites must remain stable. For this reason, it is important to determine the amount of water absorbed when the pads are allowed to stand in water and in oil. Table 3 gives water and oil absorption rates of the natural additive pads 2A and 2B and the CO commercial brake pad. The brake pads with added walnut shell additive material had an increased tendency to absorb water and oil. Ademoh and Olabisi found that water and oil absorption increased due to the increase of filler material [20]. This result was influenced by the increase in the ratio of walnut shell since the production conditions of the pads were equal. The brake pads changed in weight and size according to their tendency to absorb water and oil. This indicated that the walnut shell powder was prone to absorb water and oil due to its low dust density [29]. According to the hardness change, sample 2B exhibited the lowest density, and the sample lost the most hardness.

The changes in the mass and thickness of the tested composites are shown in Table 3. These changes were used for evaluating the thermal stability of the composites against wear. As can be seen, the wear rate of sample 2B showed loss compared to the other samples. This increase in weight loss can be explained by the porosity of the 2B sample, which had the highest water and oil absorption rate. As the porosity

Table 3 Average values of water and oil absorption rates

No.	Brake pads	Weight (%) ± 0.074	Width (%) ± 0.022	Length (%) ± 0.008	Thickness (%) ± 0.026	Hardness (%) ± 0.870
<i>Water absorption</i>						
1	2A	0.27	0.05	0.02	0.11	4.49
2	2B	0.37	0.06	0.03	0.12	5.62
3	CO	0.19	0.01	0.01	0.06	3.49
<i>Oil absorption</i>						
		±0.054	±0.047	±0.004	±0.044	±0.532
1	2A	0.43	0.16	0.02	0.11	1.14
2	2B	0.47	0.18	0.02	0.17	2.27
3	CO	0.34	0.07	0.01	0.06	1.14

increased, the friction and the weight loss of the brake pad increased due to the increase in roughness. Ghazi et al. found that as the porosity increased, the wear increased [35].

Mechanical behaviour analysis

The hardness test is an important test applied to the brake pads. Hardness is a factor that affects the friction coefficient, and in some studies, a true proportion was observed between them. However, in other studies, no correlation was found between hardness and the friction coefficient. Table 4 shows the test results of the natural additive (walnut shell dust) brake pads and the commercial pad (2A, 2B and CO).

The value of hardness was reduced because the amount of walnut dust in sample 2A was half the amount of that in the 2B sample. As the amount of walnut in the lining composition increased, the hardness also increased. Qi et al. found that the walnut shell dust content added to the brake pad increased the hardness of the brake pad [16]. The hardness value of the commercial brake pad was measured as 86 Shore D. This high hardness can be attributed to the increase in bonds. If the material is softer, the actual contact area increases and the friction coefficient becomes higher [36]. The increase in the hardness of the pad causes the wear resistance to increase [20].

The friction test was carried out under constant sliding conditions. The purpose of the test was to determine the effects of walnut shell dust on the change in the friction coefficient. The changes of the friction coefficient values of all samples were recorded during each test included in the

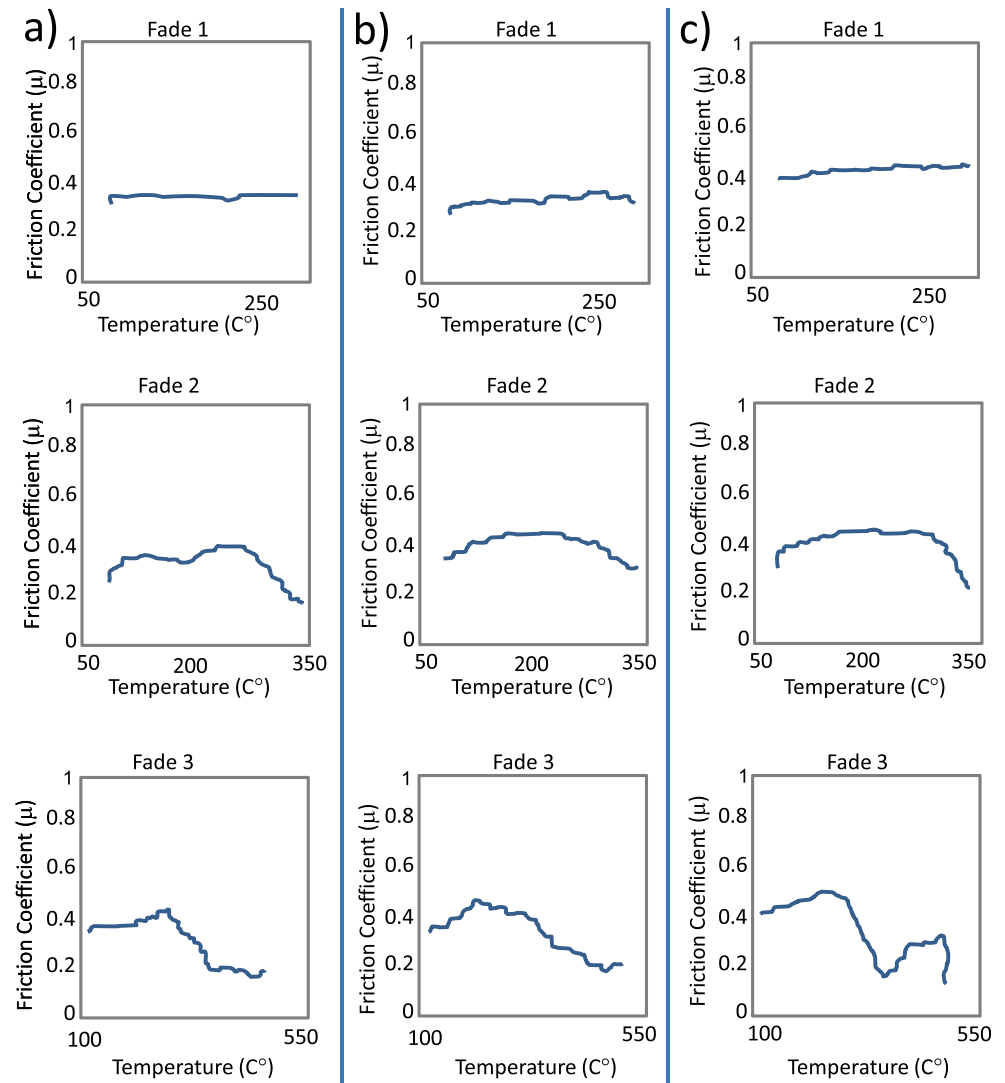
SAE-J661. During the first fade period of the Chase test (testing up to 290 °C), the friction composites showed a stable friction performance (Fig. 8). The friction coefficient was approximately 0.37, 0.37 and 0.48 for samples 2A, 2B and CO at the first recovery of the test, respectively. The friction coefficient of the CO sample was higher than the other samples (2A and 2B) for the first period of the test. However, the coefficients of friction in the graphs appear to be stable.

As can be observed from Fig. 8, all test results fell in the Fade 2 process. During the Fade 2 testing process, the friction coefficient of the 2A and CO samples were increased by increasing the temperature from 100 to 260 °C, and then decreased by increasing the temperature further to 350 °C. In the 2nd stage of recovery, the friction coefficient started to increase with decreasing temperature. According to the 2nd stage test results of the 2B sample, when the amount of walnut shell was 7%, the coefficient of friction did not show a significant increase or decrease despite the increase in temperature and progressed more steadily than with the 2A sample. It can be said that increasing the amount of walnut shell had a positive effect on the stability of the friction coefficient. At the end of the tests in Fade 3, the coefficient of friction of all samples showed a significant decrease after 300 °C. The friction coefficients in the Fade 3 phase were observed in the samples 2A and 2B as 0.138 and 0.16, respectively. Furthermore, the decreased friction coefficient was attributed to the heat fade effect [37]. The heat fade is the decrease in friction force at elevated temperatures, and it is closely correlated with thermal disintegration of the binder resin. However,

Table 4 Average values of test results of brake pad samples

No.	Brake pads	Normal friction coefficient (μ) ± 0.023	Hot friction coefficient (μ) ± 0.034	Type	Wear rate (g) ± 0.302	Hardness (Shore D) ± 0.816	Conductivity (W/mK) ± 0.164	Density (g/cm ³) ± 0.106
1	2A	0.348	0.316	EE	0.64	85	1.56	2.260
2	2B	0.399	0.400	FF	1.36	87	1.19	2.232
3	CO	0.398	0.362	FF	0.85	86	1.24	2.470

Fig. 8 Fade graphs of the friction coefficient test for the test specimen brake pads: **a** 2A; **b** 2B; **c** CO



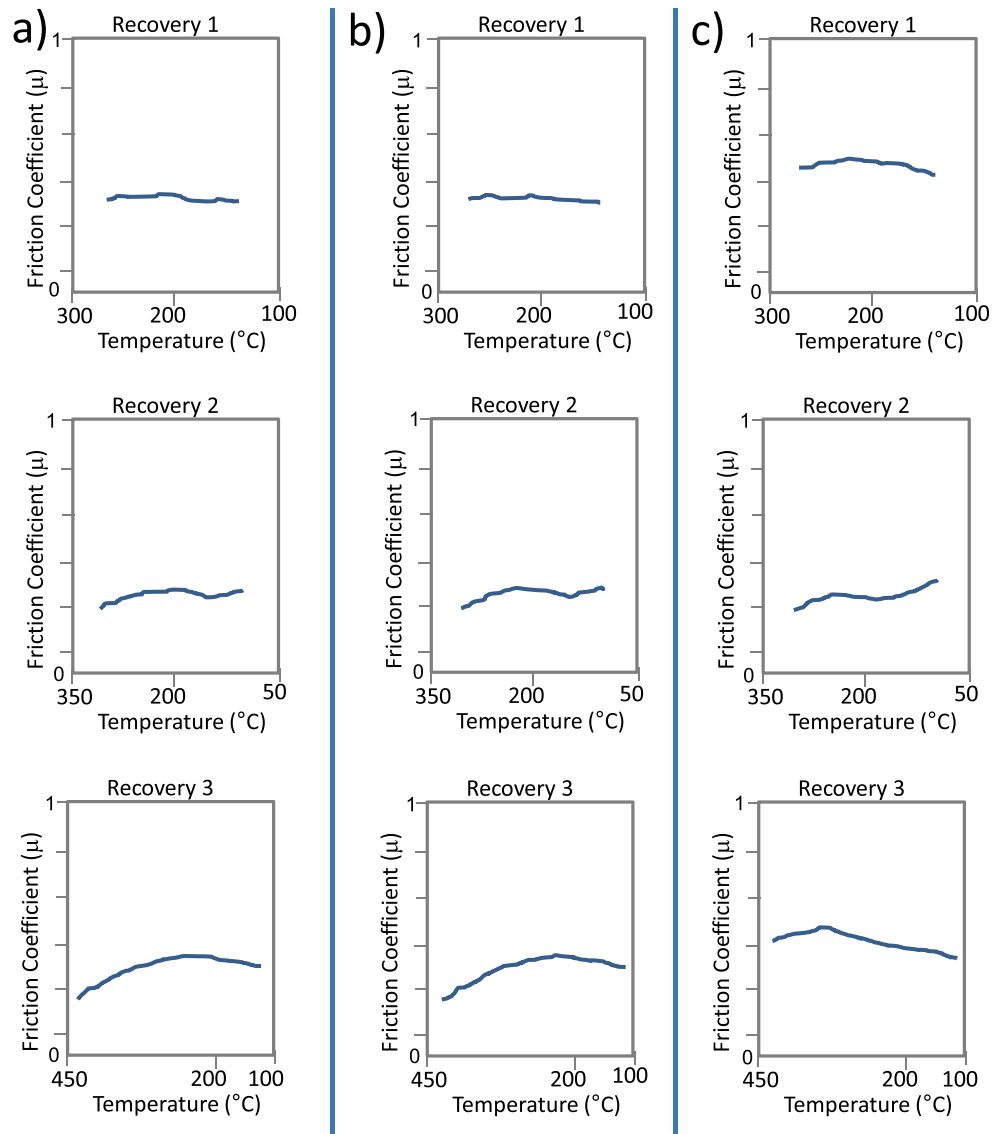
the temperatures in this interval were higher than the decomposition temperature of lignin, as the main constituent of walnut shell dust, which is 160 °C [16]. In the third round of recovery (Fig. 9), the most stable friction coefficient was obtained in 2B. This fact could be attributed to the presence of lignin, whose slight decreasing rate and lubrication properties were responsible for stabilising the coefficient of friction (COF) values of 2A and 2B. The walnut shell lignin content was increased and thus could have been used as an effective lubricant which suppressed the fade phenomenon of the final composite during friction test at elevated temperatures.

The hot and cold friction coefficients of the 2A, 2B and CO samples are given in Table 5. According to the results of the tests, the average normal (cold) friction coefficients were found as 0.348, 0.399 and 0.398 in 2A, 2B and CO samples, respectively. The friction coefficient values of the 2B sample and the commercial CO pads were very close to each other. The hot friction coefficients were 0.316, 0.400 and 0.362 μ in 2A, 2B and CO, respectively. The highest value for the hot

friction coefficients was obtained from the 2B sample. It can be said that the walnut additive helped to increase the friction coefficient.

The friction coefficient must be kept at a balanced level at a wide range of temperatures, loads and speeds [38]. The 3D surface graph of the friction coefficients observed at 100 brakings is given in Fig. 10. The friction coefficient values of samples 2A, 2B and CO measured after 100 brakings were obtained as 0.334, 0.425 and 0.332, respectively. According to the graphs, 2A (Fig. 10a) and the commercial CO pad had similar values. As the number of applications in the 2A and CO samples increased, the coefficient of friction decreased. On the other hand, for the 2B specimen (Fig. 10b), the friction coefficient increased as the application increased at low friction forces. However, the coefficient of friction became more stable with increasing friction force. As the number of applications increased, the coefficient of friction increased in the 2B sample in which the walnut additive ratio was increased to 7%. In addition, the increase in friction force made the

Fig. 9 Recovery graphs of the friction coefficient test for the test specimen brake pads: **a** 2A; **b** 2B; **c** CO



coefficient of friction more stable. This can be explained by the increase in the percentage of walnut shell. The walnut shell structure is oily and in fact, in order to achieve friction stability for a wide range of temperatures, commercial friction materials often contain two or more solid lubricants and friction modifiers [39]. The walnut shell was used as a friction modifier and lubricant in the 2B sample instead of petrocok.

Table 5 Average values of hot and cold friction coefficients of 2A, 2B and CO samples

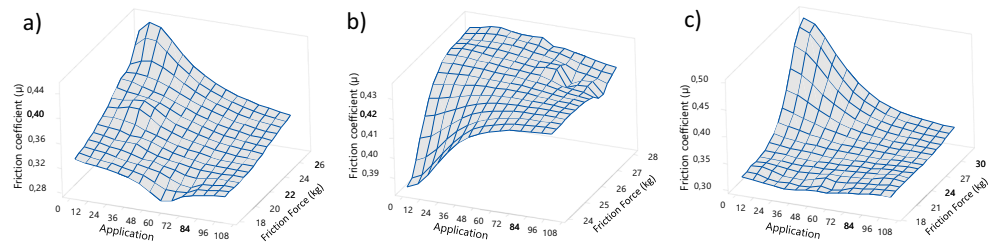
No.	Sample	Cold COF (μ) $\pm 0,023$	Hot COF (μ) $\pm 0,034$	Class
1	2A	0.348	0.316	EE
2	2B	0.399	0.400	FF
3	CO	0.398	0.362	FF

Therefore, the walnut shell fulfilled the task of petrocok and showed better braking performance.

The wear rates of the 2A, 2B and CO samples are shown in Table 6. With the abrasion value of 1.36 g, the 2B sample was the most abrasive pad sample. The reason for this was that the coefficient of friction was high and the walnut shell content was higher than in sample 2A. A more stable friction coefficient graph was obtained by increasing the amount of walnut shell, and the wear amount of the pad increased.

It can also be said that the thermal conductivity of the 2B specimen was lower than that of the other pads, resulting in an increase in the amount of wear depending on the temperature. When looking at the results, an accurate ratio can be seen between the wear and hardness, but this relationship may not always be directly proportional. Jaafar et al. in their work could not obtain a true ratio between wear and hardness [40]. The wear rate of 2A, which contained less walnut shell,

Fig. 10 Friction coefficients at 100 brakings: **a** 2A; **b** 2B; **c** CO



was lower than that of CO and 2B. It can be said that the amount of walnut added to the pad composite made an observable change on the amount of wear. The wear rate was calculated using the formula in Eq. (2).

$$W = \frac{1}{2\pi R} \times \frac{1}{f_m^n} \times \frac{m_1 - m_2}{\rho} \quad (2)$$

where n is the revolution of the rotating disk, m_1 and m_2 are the average weights of samples before and after the test (g), W is the specific wear rate (cm^3/Nm), R is the radius of the sample (m) and ρ (density of the sample) and f_m is the average friction force (N).

Conclusions

The friction composites combined with walnut shell were designed, fabricated and characterised for physical, mechanical, thermo-mechanical and tribo-performance. The assessment of braking performance was carried out on a Chase-type friction testing machine using the standard test protocol conforming to the SAE J661 regulation. The physical and mechanical characteristics of the composites were evaluated as being fit within industrial norms. The influence of the walnut shell dust component on the mechanical, frictional, thermal and wear behaviours of the brake friction materials was investigated and the conclusions are summarised as follows:

- New formulations for automotive brake pads with additions of walnut shell dust (2A and 2B) were successfully manufactured.
- Brake pads with 3.5 (2A) and 7% (2B) walnut shell dust produced with walnut shell dust exhibited performances comparable to commercial linings and in conformance with standards.

Table 6 Average values of wear rate of samples

Sample	2A	2B	CO
Wear rate (g)	0.64	1.36	0.85
Wear rate change (%)	0.10	0.20	0.20

- As the amount of walnut shell (3.5 (2A) and 7% (2B)) in the pad composition increased, the hardness value also increased. The results were close to the hardness value of the commercial brake pad (CO) sample (86 Shore D). The hardness increased very little when the walnut shell was used as an alternative to petroleum coke.
- As the amount of walnut shell increased, the density value decreased. The decrease in density with the increased amount of walnut shell dust was explained by the lower density of the pad related to high porosity.
- Thermal conductivity results were within the standard limits according to ASTM-E1461–01. Increasing the ratio of walnut shell reduced the thermal conductivity within acceptable limits.
- The brake pads with walnut shell as a natural additive material had an increased tendency to absorb water and oil. Water and oil absorption in all samples was between approximately 0.2 and 0.4%. This value indicated that the water and oil absorption rates of the brake pads were acceptable.
- The walnut shell dust was homogeneously dispersed within the microstructure. The walnut shell dust structure in the composite was fibrous.
- The fade performance increased with the increase in the walnut shell content, whereas the recovery performance always remained higher than 100% and was observed to stabilise with the increase in walnut shell content.
- The highest value for the hot friction coefficient was obtained with the 2B sample. The walnut shell additive caused increase in the friction coefficient.
- According to the SAE J661 standard, the friction coefficient results of the brake pads were obtained as EE for the 2A and as FF for the 2B and CO samples. All letter symbols found were in accordance with the standards and fell within an acceptable range.
- Depending on the weight loss, the maximum amount of wear was seen on the 2B sample. This increase in weight loss can be explained by the porosity of the 2B sample, which had the highest water and oil absorption rate.
- The performance of the brake pads (2A and 2B) conformed to the standards.

Funding Information This study was supported by the Scientific Research Project Unit of Duzce University (DÜBAP-2015/72). The authors also thank Balataclar Cooperation Inc. for their contributions.

References

- Rashid, B., Leman, Z., Jawaaid, M., Ghazali, M., Ishak, M., Abdelgnei, M.: Dry sliding wear behavior of untreated and treated sugar palm fiber filled phenolic composites using factorial technique. *Wear*. **380**, 26–35 (2017)
- Kchaou, M., Lazim, A.M., Hamid, M.A., Bakar, A.A.: Experimental studies of friction-induced brake squeal: influence of environmental sand particles in the interface brake pad-disc. *Tribol. Int.* **110**, 307–317 (2017)
- Menapace, C., Leonardi, M., Perricone, G., Bortolotti, M., Straffelini, G., Gialanella, S.: Pin-on-disc study of brake friction materials with ball-milled nanostructured components. *Mater. Des.* **115**, 287–298 (2017)
- Hong, U.S., Jung, S.L., Cho, K.H., Cho, M.H., Kim, S.J., Jang, H.: Wear mechanism of multiphase friction materials with different phenolic resin matrices. *Wear*. **266**(7–8), 739–744 (2009). <https://doi.org/10.1016/j.wear.2008.08.008>
- Weintraub, M.: Brake additives consultant. Private communication 107–127 (1998).
- Zaharudin, A., Talib, R., Berhan, M., Budin, S., Aziurah, M.: Taguchi method for optimising the manufacturing parameters of friction materials. *Proceedings of Regional Tribology Conference 2011: RTC2011*, 246 (2011)
- Eriksson, M.: Friction and contact phenomena of disc brakes related to squeal. *Citeseer* (2000)
- Aigbodion, V.S., Akadike, U., Hassan, S.B., Aduke, F., Agunsoye, J.O.: Development of asbestos-free brake pad using bagasse. *Trib Ind.* **32**(1), 12–18 (2010)
- Jacko, M.G., Tsang, P.H.S., Rhee, S.K.: Automotive friction materials evolution during the past decade. *Wear*. **100**(1–3), 503–515 (1984). [https://doi.org/10.1016/0043-1648\(84\)90029-2](https://doi.org/10.1016/0043-1648(84)90029-2)
- Blau, P.J.: Compositions, Functions, and Testing of Friction Brake Materials and their Additives. Oak Ridge National Lab., Oak Ridge (2001)
- Idris, U., Aigbodion, V., Abubakar, I., Nwoye, C.: Eco-friendly asbestos free brake-pad: using banana peels. *J K Saud Un Eng Sci* **27**(2), 185–192 (2015)
- Lazim, A.M., Kchaou, M., Hamid, M.A., Bakar, A.A.: Squealing characteristics of worn brake pads due to silica sand embedment into their friction layers. *Wear*. **358**, 123–136 (2016)
- Aku, S., Yawas, D., Madakson, P., Amaren, S.: Characterization of periwinkle shell as asbestos-free brake pad materials. *Pac. J. Sci. Technol.* **13**(2), 57–63 (2012)
- A. O. A. Ibadode, Dagwa, i.M.: Development of Asbestos-Free Friction Lining Material from Palm Kernel Shell. *J. of the Braz. Soc. of Mech. Sci. & Eng.* xxx(2), 166–173 (2008)
- Ghazali, C.M.R., Kamarudin, H., Shamsul, J., Abdullah, M., Rafiza, A.: Mechanical properties and wear behavior of brake pads produced from palm slag. *Adv Mat Res* **341**(26), 26–30 (2012)
- Qi, S., Fu, Z., Yun, R., Jiang, S., Zheng, X., Lu, Y., Matejka, V., Kukutschova, J., Peknikova, V., Prikasky, M.: Effects of walnut shells on friction and wear performance of eco-friendly brake friction composites. *P I Mech Eng J-J-Eng.* **228**(5), 511–520 (2014). <https://doi.org/10.1177/1350650113517112>
- El-Tayeb, N.S.M., Liew, K.W.: On the dry and wet sliding performance of potentially new frictional brake pad materials for automotive industry. *Wear*. **266**(1–2), 275–287 (2009). <https://doi.org/10.1016/j.wear.2008.07.003>
- Solomon, D.G., Berhan, M.N.: Characterization of Friction Material Formulations for Brake Pads. In: *World Congress on Engineering*, pp. 2–4 (2007)
- Mutlu, I., Oner, C., Findik, F.: Boric acid effect in phenolic composites on tribological properties in brake linings. *Mater. Des.* **28**(2), 480–487 (2007). <https://doi.org/10.1016/j.matdes.2005.09.002>
- Ademoh, N.A., Olabisi, A.I.: Development and evaluation of maize husks (asbestos-free) based brake pad. *Ind Eng Let* **5**(2), 67–80 (2015).
- Saffar, A., Shojaei, A.: Effect of rubber component on the performance of brake friction materials. *Wear*. **274–275**, 286–297 (2012). <https://doi.org/10.1016/j.wear.2011.09.012>
- Prabhu, T.R.: Effects of solid lubricants, load, and sliding speed on the tribological behavior of silica reinforced composites using design of experiments. *Mater. Des.* **77**, 149–160 (2015). <https://doi.org/10.1016/j.matdes.2015.03.059>
- Ram Prabhu, T., Varma, V.K., Vedantam, S.: Tribological and mechanical behavior of multilayer cu/SiC + gr hybrid composites for brake friction material applications. *Wear*. **317**(1–2), 201–212 (2014). <https://doi.org/10.1016/j.wear.2014.06.006>
- 570–98, A.D.: Standard test method for water absorption of plastics. In. (1999)
- ASTM: standard test method for acetone extraction of phenolic molded or laminated products. In: *ASTM D 494–04*. pp. 1–3. ASTM International, US (2004)
- J661, S.: Brake lining quality test procedure. In, vol. J661. (2012)
- Dadkar, N., Tomar, B.S., Satapathy, B.K.: Evaluation of flyash-filled and aramid fibre reinforced hybrid polymer matrix composites (PMC) for friction braking applications. *Mater. Des.* **30**(10), 4369–4376 (2009). <https://doi.org/10.1016/j.matdes.2009.04.007>
- Lu, Y.: A combinatorial approach for automotive friction materials: effects of ingredients on friction performance. *Compos. Sci. Technol.* **66**(3), 591–598 (2006)
- Ertan, R., Yavuz, N.: An experimental study on the effects of manufacturing parameters on the tribological properties of brake lining materials. *Wear*. **268**(11–12), 1524–1532 (2010). <https://doi.org/10.1016/j.wear.2010.02.026>
- G. Akıncıoğlu, H.Ö., I. Uygur, S. Akıncıoğlu: Determination of Friction-Wear Performance and Properties of Eco-Friendly Brake Pads Reinforced with Hazelnut Shell and Boron Dusts. *Arab J Sci Eng* **43**(9), 4727–4737 (2018).
- Singh, T., Patnaik, A., Chauhan, R.: Optimization of tribological properties of cement kiln dust-filled brake pad using grey relation analysis. *Mater. Des.* **89**, 1335–1342 (2016). <https://doi.org/10.1016/j.matdes.2015.10.045>
- Yawas, D.S., Aku, S.Y., Amaren, S.G.: Morphology and properties of periwinkle shell asbestos-free brake pad. *J K Saud U Eng Sci* **28**(1), 103–109 (2016). <https://doi.org/10.1016/j.jksues.2013.11.002>
- Bijwe, J., Kumar, M.: Optimization of steel wool contents in non-asbestos organic (NAO) friction composites for best combination of thermal conductivity and tribo-performance. *Wear*. **263**(7–12), 1243–1248 (2007). <https://doi.org/10.1016/j.wear.2007.01.125>
- Blau, P.J., McLaughlin, J.C.: Effects of water films and sliding speed on the frictional behavior of truck disc brake materials. *Tribol. Int.* **36**(10), 709–715 (2003). [https://doi.org/10.1016/S0301-679X\(03\)00026-4](https://doi.org/10.1016/S0301-679X(03)00026-4)
- Ghazi, A., Chandra, K., Misra, P.: Development and characterization of Fe-based friction material made by hot powder preform forging for low duty applications. *J. Miner. Mater. Charact. Eng.* **10**(13), 1205–1212 (2011)
- Stadler, Z., Krmel, K., Kosmac, T.: Friction behavior of sintered metallic brake pads on a C/C–SiC composite brake disc. *J. Eur. Ceram. Soc.* **27**(2–3), 1411–1417 (2007). <https://doi.org/10.1016/j.jeurceramsoc.2006.04.032>
- Ji, Z., Jin, H., Luo, W., Cheng, F., Chen, Y., Ren, Y., Wu, Y., Hou, S.: The effect of crystallinity of potassium titanate whisker on the tribological behavior of NAO friction materials. *Tribol. Int.* **107**, 213–220 (2017)

38. Erikssona, M., Lordb, J.: Jacobson, S.: Wear and contact conditions of brake pads: dynamical in situ studies of pad on glass. *Wear*. **249**, 272–278 (2001)
39. Martinez, A.M., Echeberria, J.: Towards a better understanding of the reaction between metal powders and the solid lubricant Sb₂S₃ in a low-metallic brake pad at high temperature. *Wear*. **348–349**, 27–42 (2016). <https://doi.org/10.1016/j.wear.2015.11.014>
40. Jaafar, T.R., Selamat, M.S., Kasiran, R.: Selection of Best Formulation for Semi-Metallic Brake Friction Materials Development. In: Powder Metallurgy. InTech (2012)

Publisher's note Springer Nature remains neutral with regard to jurisdictional claims in published maps and institutional affiliations.